

NATO Science Fellowship Programme

Final report about activities in the frame of the
Agreement No. 2(2001)

in the period June 1st 2001- May 31st, 2002

Title: Diagnostics of new ecological materials

by Dr Iraida Bountseva

Host institution in the Czech republic: **Nuclear Research Institute, Řež**

Approved by

Head of the Central Analytical Laboratory:

RNDr. Z.Málek, CSc

The Nuclear research Institute Řež is a leading research institute of the Czech republic in the field of nuclear research, especially related to the solution of the problems of the safe treatment, storage and disposal of hazardous radionuclides, originating from nuclear facilities as well as hazardous compounds and elements in the waste originating from chemical industry.

During my research stay in the frame of the NATO Science Fellowship Program I participated in the research work of the team of the Nuclear Research Institute Řež (Head of the team Dr V.Balek) in cooperation with the researchers from the Institute of Inorganic Chemistry AS CR Řež. The research team headed by Dr. V. Balek has been engaged in the design and diagnostics of several new materials for the application in the environmental technologies.

The objective of my research was to participate in the preparation and characterization of new ecological materials, such as advanced titanium dioxide based photocatalysts, ruthenium oxide based catalysts, as well as aluminium oxide based adsorbents and catalysts. Moreover, specially designed glasses and ceramics for immobilization of hazardous wastes were investigated in order to characterize their chemical durability and thermal stability.

In the research work various instrumental methods were used for the diagnostics of the new ecological materials and their precursors. The unique method, like diffusion structural analysis (DSA), developed originally in the NRI Řež, has been used in order to characterize changes of the microstructure of the precursors for the new materials during their thermal treatment. A recently designed mathematical model was recently used for the evaluation of the DSA results and prediction of the properties of the materials investigated

Thermal analysis methods, such as thermogravimetry, differential thermal analysis coupled with evolved gas analysis by mass spectrometry were used in order to characterize the chemical processes taking place during thermal treatment of the materials precursors The X-ray diffraction and Scanning electron microscopy were used to support the interpretation of the results obtained.

Diffusion structural analysis (DSA)

DSA is based on the measurement of radon release rate from samples previously labeled. The samples for DSA measurements were labeled using absorption of ^{228}Th and ^{224}Ra radionuclides from acetone solution. The specific activity of the sample was 10^5 Bq per gram. The labeled samples were stored three weeks prior to the DSA measurements in dry conditions to allow the radioactive equilibrium between the ^{228}Th and ^{224}Ra nuclides to be established.

Thorium nuclide ^{228}Th (half-life 1.9 years) used for labeling samples serves as a quasi-permanent source of radon ^{220}Rn (half-life 55 s). Atoms of radon ^{220}Rn are formed by the spontaneous α -decay of ^{228}Th and ^{224}Ra . The half-life of ^{220}Rn ensures that the steady state between ^{224}Ra and ^{220}Rn is established within several minutes, which makes it possible to investigate even rapid changes in the solids and on their surface. Radon formed by the spontaneous γ -decay of ^{228}Th absorbed on the sample surface.

The recoil depths of ^{224}Ra and ^{220}Rn ions implanted by the recoil energy (85 keV/atom) into the samples were calculated by means of the TRIM code. Therefore, we can suppose that the radon atoms penetrated into the near surface layers to a maximum depth of 80 nm.

The release rate of radon from the sample, called also emanation rate, E, can be expressed in a simplified way as follows:

$$E = E_{\text{Recoil}} + E_{\text{Diffusion}} = E_{\text{Recoil}} + D(T) \cdot \Psi(T) \quad (1)$$

Where E_{Recoil} is depending on external surface area and radon recoil path in the respective solid, $E_{\text{Diffusion}}$ is depending on the number of the diffusion paths serving for the gas release, $D(T)$ is characterizing the radon diffusion permeability of transporting paths and $\Psi(T)$ is characterizing the microstructure changes in the solid.

The function $\Psi(T)$ was suggested for the description of the change of number of defects, which can serve as traps for radon atoms. The number of radon diffusion paths is changing during heating of the sample.

In the modelling of the DSA curves it was suggested to use the product $D(T) \cdot \Psi(T)$ for the description of the changes of the emanating rate due to radon diffusion in the sample where annealing of the defects, phase changes or other solid state transitions take place. In this case the function $\Psi(T)$ reflects the change of the number of radon diffusion paths during heating. The function $D(T)$ – reflects the change of radon diffusion permeability of the average radon transport path. Thus product $D(T) \cdot \Psi(T)$ represents change of radon permeability in all diffusion paths participating in process.

If solid state transitions in bulk of materials take place, a series of intermediate metastable structures may be formed, considerably varying in the number of radon migration paths, in the permeability of radon diffusion paths as well as in the area of surface accessible for gas release. It was observed, that these processes essentially influenced the shape of the DSA-curve. If several consecutive solid-state changes take place during sample heating, several peaks may be observed on the DSA-curve. In order to evaluate the DSA results obtained during heating of such solids, different mechanisms for radon diffusion were considered.

The temperature dependencies of radon diffusion coefficient $D_n(T)$ can be considered as growing functions, whereas the $\Psi_n(T)$ (determining the annealing of diffusion paths) as descending functions. Consequently, peak-like parts are resulting in the mathematical modelling of the temperature dependencies of emanating rate E .

In general, the shape of the DSA results reflect the number of diffusion paths serving for the gas release; $D(T)$ is the function characterising the permeability of the transporting paths and $\Psi(T)$ the function characterising the microstructure changes in the solids. The $D(T)$ and $\Psi(T)$ functions used in the modelling can be used for the characterization of the solid state processes taking pace in the solid during heating.

Theoretical background of the DSA results evaluation.

Mathematical equations presented in Eq.(2)-(5) were used in the evaluation of the DSA experimental results. The dependences of the structure function $\Psi(T)$ and $d\Psi/dT$ were used in order to characterize the annealing of near surface layers irregularities serving as diffusion paths for radon.

$$E_{\Sigma}(T) = B(T) + D(T) \quad (2)$$

where $B(T) = E(T) \cdot \Psi(T)$,

$$E(T) = p_3 \cdot p_1 \cdot \exp\left(-\frac{p_2}{T}\right) \cdot \left[\coth\left(\frac{3}{p_1 \cdot \exp\left(-\frac{p_2}{T}\right)}\right) - \frac{p_1 \cdot \exp\left(-\frac{p_2}{T}\right)}{3} \right], \quad (3)$$

$$\Psi(T) = 1 - 0.5 \left[1 + \operatorname{erf} \left(\frac{T - p4}{\sqrt{2 \cdot p5}} \right) \right] \quad (4)$$

$$D = p6 \cdot \exp \left(-\frac{p7}{T} \right), \quad (5)$$

Parameters $p1...p7$ were determined during the fitting of the model curves with the experimental DSA results.

Results

Thermal behaviour of titanium dioxide thin layers during heating in various gas environments.

Titania layers to be used as photocatalysts for the elimination of environmental pollutants or water decomposition were deposited on silica fused glass plate by using sol gel spin coating technique. The thermal treatment of the deposited layers was used to remove solvents and organic molecules of the precursors and to anneal structure irregularities in order to obtain durable layers with tailored properties. Some investigators suggested to introduce selected elements, such as Zn, Mn, Fe, Cr, V into the titania layers by ion bombardment aiming to improve the photosensitive properties. In the recent study Oyoshi and co workers characterized the structure, optical absorption and electronic states of Zn^{+} -ion implanted sol-gel anatase films subsequently annealed to 800 °C in nitrogen or oxygen, resp.

It was of interest to investigate the effect of heating in different gas environments (argon and oxygen) as well as the affect of Zn^{+} ions bombardment on microstructure development of the porous titania films prepared by sol gel technique.

Surface area development and microstructure changes of the samples were characterized by means of DSA under *in situ* conditions of the heating in a controlled gas environment. A good agreement between the results of DSA, TG, DTA, XRD and other methods was found. The results of DSA were evaluated by means of a theoretical model developed for this purpose and are discussed in comparison with the results of XRD and SEM.

(a) Effect of the gas environment (argon, oxygen) on the microstructure development of porous titania films on heating

We assumed that the increase of the radon release rate, E, in the temperature range 50-250 °C was controlled by the diffusion of radon along irregularities in the surface and very near surface layers. The random single jump diffusion mechanism of radon was supposed to take place in this temperature range. From the reduced slope of the increase in this temperature range we assumed that the titania film sample heated in oxygen (curve 2, Fig.1) possessed lower content of the near surface structure irregularities in comparison with the sample heated in argon (curve 1, Fig.1).

The decrease of E observed on both curves in Fig. 1 in the range 255-700 °C was ascribed to the annealing of structure irregularities and porosity of the titania films in the respective gas environment. This is in agreement with the measurement of the thickness of titania films heated to 800°C. The enhanced annealing of the structure defects during heating in oxygen

was supposedly due to the stoichiometric reconstruction of surface and near surface layers of titania film.

The enhanced release of radon observed in the temperature range above 750°C indicated the onset of the radon diffusion in bulk. From this temperature the growth of the titania grains and sintering of the layer can be expected.

The break on the DSA curve observed above 870°C was therefore ascribed to the grain growth in the interior region of the anatase structure layer, resulting in the decrease of structure defects concentration, which served as diffusion channels for radon atoms. The SEM micrographs (Fig. 2) and XRD patterns (Fig 3) confirmed this interpretation of the DSA results.

In the mathematical model used for the evaluation of the DSA results the expressions proposed recently by Beckman and Balek were used. The model curves $\Psi(T)$ characterizing the temperature dependences of the annealing of structure irregularities which served as radon diffusion paths on heating of porous titania films in argon and oxygen are presented in Fig .1 as curves 1' and 2', respectively .The comparison of the $\Psi(T)$ functions characterizing the effect of gas environment on the annealing of near surface structure irregularities is presented separately Fig 4.

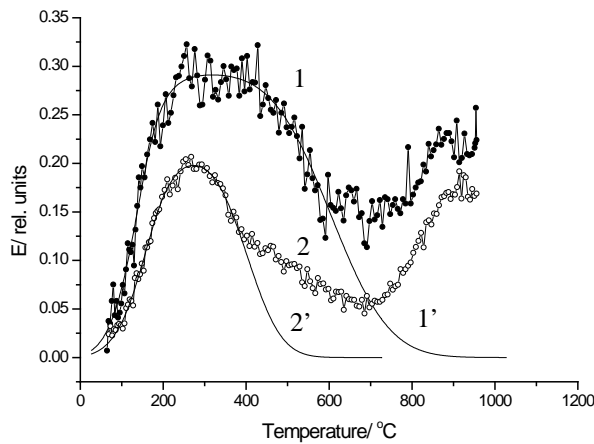
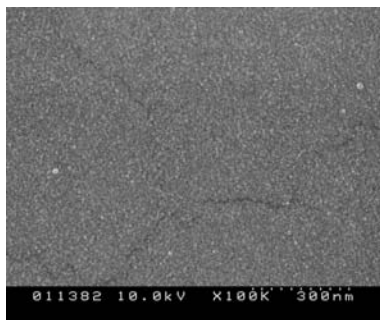
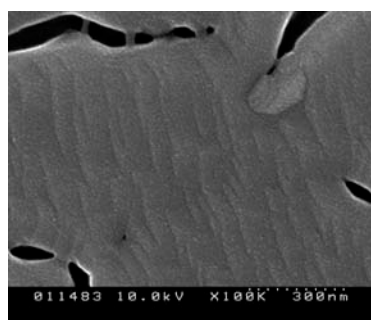


Fig. 1 DSA results of porous titania films measured on heating in argon (curve 1) and oxygen (curve 2) compared with the results of mathematical modeling (curves 1' and 2'), respectively.



a)



b)

Fig. 2 SEM micrographs of porous titania films (a) as baked at 500 °C and (b) heated to 900 °C.

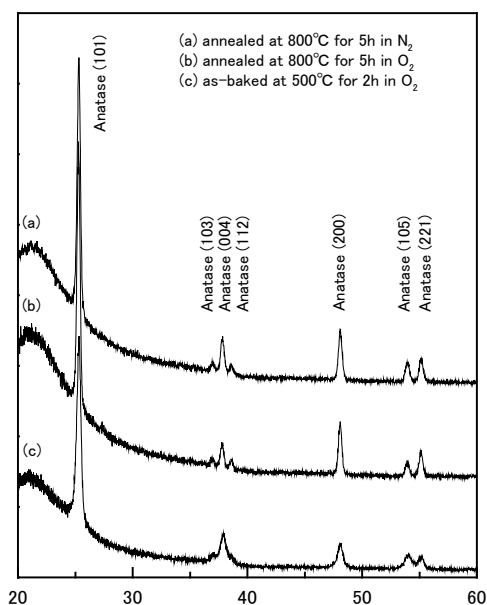


Fig. 3 XRD patterns of the titania films heated to various temperatures.

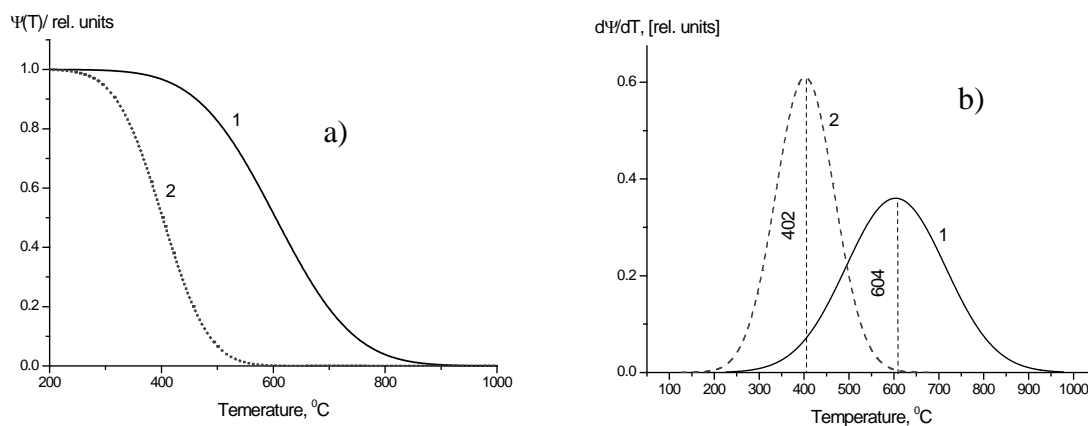


Fig. 4 Temperature dependences of (a) function $\Psi(T)$ and (b) derivative function $d\Psi/dT$, which were used for the characterization of the annealing of near surface irregularities serving as radon diffusion paths in titania films on heating in argon (curve 1) and oxygen (curve 2).

(b) Effect of Zn ions bombardment on the titania films microstructure on heating in argon and oxygen, respectively.

It was observed that Zn⁺ ions bombardment led to the increase of the density of the anatase layer to the penetration depth of the ions (50nm). The cracks evolution by Zn⁺ ions bombardment observed by SEM (Fig 5) is probably due to the tensile stress of the anatase film caused the densification of the implanted depth region.

ZnTiO₃ was observed by XRD pattern in the Zn⁺ ions bombarded titania sample after heating above 800°C in oxygen. It was supposed that the provided oxygen contributed to oxidize the implanted Zn⁺ and to form ZnTiO₃. It stabilized the implanted Zn⁺ in its lattice. The DSA results presented in Fig. 6 a, b characterize the differences in the thermal behavior of the titania film samples treated by Zn⁺ ions implantation on heating in argon and oxygen, respectively.

In Fig.6 the reduced slope of the DSA curve of the Zn^{+} -ion bombarded titania film (curve 2) was observed in temperature range 50-250°C, which indicated that the titania layer after Zn^{+} - bombardment became more compact and the number of microstructure irregularities serving as paths for radon atoms in the near surface layers decreased. The annealing of porosity, resulting in the initial densification of the sample, was characterized by the decrease of the radon release rate, E, in the temperature range 260 -820°C.

The enhanced release of radon observed on heating above 830°C indicated the onset temperature where the radon diffusion in bulk took place. The break observed on the DSA curve at 920°C was ascribed to the sintering and the growth of titania particles. This temperature was somewhat higher than that observed when the non-implanted titania film was heated in argon (see Fig.6a, curve 1). It is in agreement with our hypothesis, that the Zn^{+} ions implantation led to the increased density of the titania layer, consequently to the decrease of its sinterability on heating to the temperatures above 800°C.

Moreover, when comparing the curves 1 and 2 in Fig.6b we assumed that the presence of oxygen has been enhancing the annealing process in this temperature range.

The $\Psi(T)$ functions corresponding to the Zn^{+} implanted film when heated in argon and oxygen are presented in Fig 7a, b as curves 2. It is obvious that the presence of oxygen facilitated the annealing of the titania film in the range 270-600°C. However in the range 600-700°C it was slowed down, probably due to the formation of Zn-titanate. This hypothesis was confirmed by the E increase above 710°C, corresponding supposedly to the enhanced radon diffusion along newly formed Zn-titanate interfaces, serving as diffusion paths for radon.

Fig.8 a,b depicts the DSA experimental results of the Zn^{+} - ion bombarded titania , characterized the differences in the structure development of the samples ,where $ZnTiO_3$ has been formed on heating in argon and oxygen ,respectively. In these figures we present the comparison of the DSA experimental results (curve 1) and the remainder (curve 2) after subtraction of the model curves, characterizing the annealing of the irregularities and the bulk diffusion of radon et elevated.

The advantageous use of the DSA consisted in the possibility to reveal the annealing of the structure irregularities in the near surface layers of anatase, serving as diffusion paths for inert (radon), which was introduced prior to the measurement into the surface layers of the investigated samples.

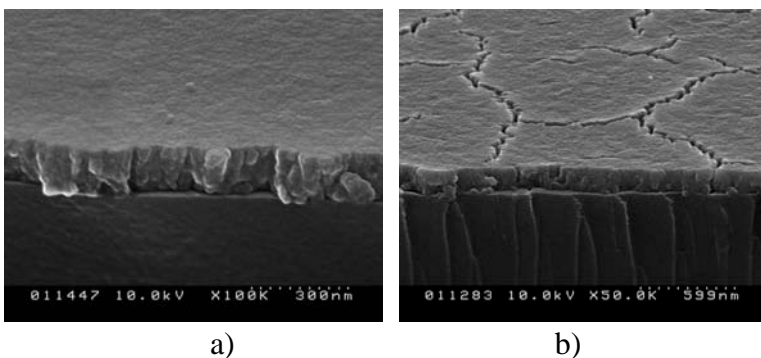


Fig. 5 SEM micrographs of titania films baked at 500 °C made (a) before the ion bombardment and (b) after the 100 keV Zn^{+} ions bombardment.

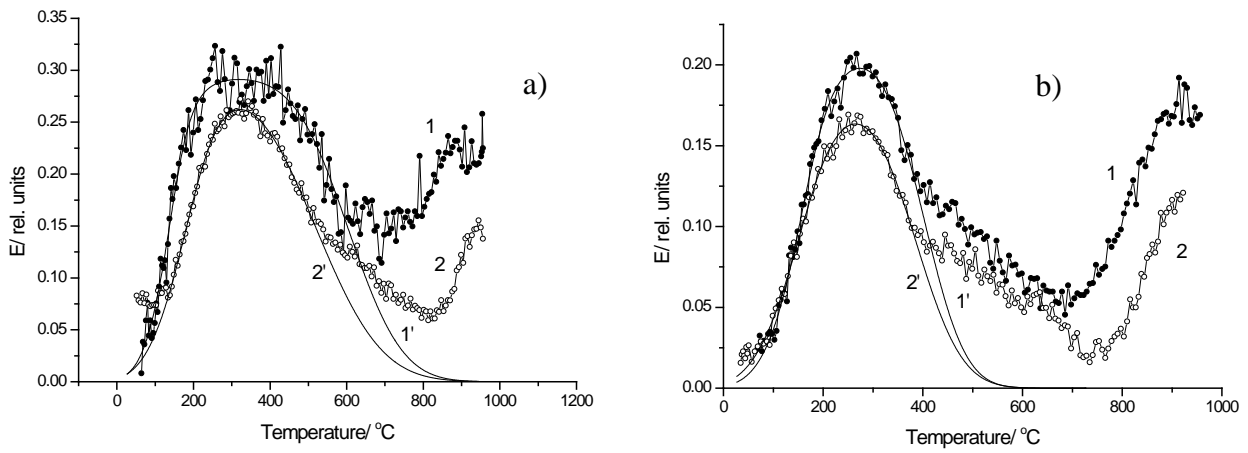


Fig. 6 Comparison of DSA results of non implanted and Zn⁺ ion implanted titania films on heating (a) in argon and (b) in oxygen . Curve 1 and 2 correspond to the non- bombarded and Zn⁺ ion bombarded films, respectively. Curves 1' and 2' correspond to the respective model curves.

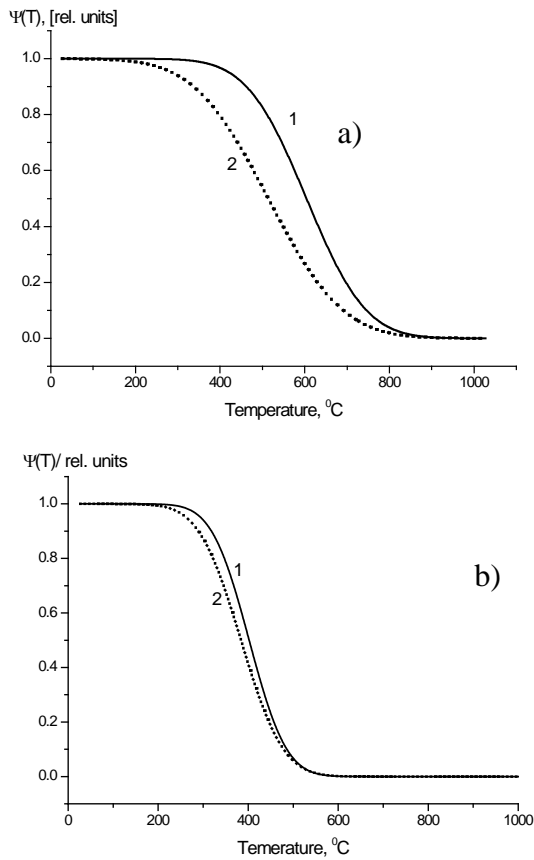


Fig. 7 Temperature dependences of the $\Psi(T)$ function, which were used for the characterization of the annealing of near surface irregularities in titania films on heating in argon (a) and oxygen (b). Curve 1 and 2 correspond to the non- bombarded and Zn⁺ ion bombarded films, respectively

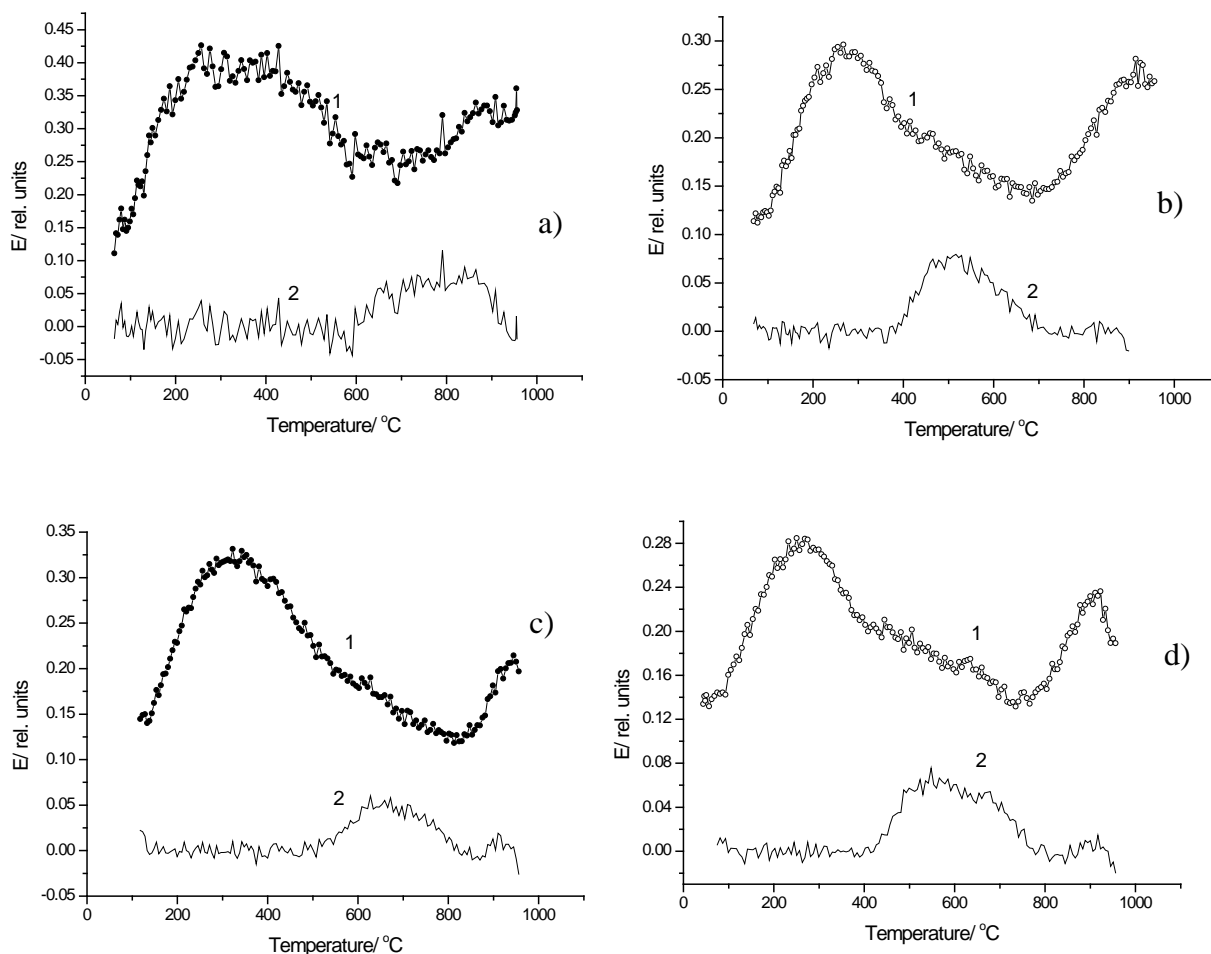


Fig. 8 Comparison of the DSA experimental results of titania films (curve 1) and the remainder curves (curve 2) resulting after subtraction of the model curves, characterizing the annealing of the near surface irregularities and the bulk diffusion of radon et elevated temperatures: (a) and (b) non- bombarded titania films heated in argon and oxygen, respectively (c) and (d) Zn^{2+} - ion bombarded titania films on heating in argon and oxygen, respectively.

Preparation and characterization of mesoporous titanium dioxide gels

Mesoporous TiO_2 gels, which are attractive for their potential application to photocatalysts and electrodes for wet solar cells have been prepared by a newly developed method and their microstructure was investigated. Monolithic gels were obtained by hydrolysis of $Ti(n-C_4H_9O)_4$ in an ethanol/ethylacetoacetate solution. The wet gels were aged and dried after immersion in an ethanol solution of surfactants, cetyltrimethylammonium chloride (CTAC) or benzyltrimethylammonium chloride (BTAC) (CTAC- or BTAC-modified xerogels). The organic substances in the gels were removed by heating up to $560^\circ C$ in air. After calcination at $600^\circ C$, the characterization by DSA and N_2 -adsorption measurements were made. The BET surface area, the pore volume and the pore size increased as a result of surfactant modification. The most probable pore radius of the xerogel, BTAC-modified gels and CTAC-modified gel was 2.4, 2.8 and 5.0 nm, respectively.

It was found that the pore size distribution of mesoporous TiO_2 gels depends on the size of surfactant micelles. The microstructure of mesoporous gels was characterized by DSA. Differences in the Rn -release rate of the samples during heating were found, and the porosity increased in the following sequence: xerogel < BTAC-modified gel < CTAC-modified gel. The Rn release rate depends on the pore size of the gels as well as the surface areas.

Thermal stability of the meso-porous powders was evaluated from the DSA results using the mathematical model.

(a) Surface modified titania gel powders

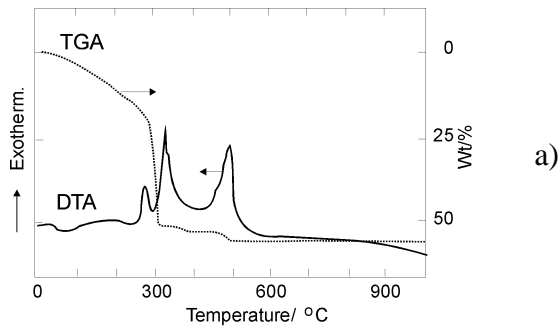
Surface modified titania powders were prepared from the hydrolyzed alcoxide precursors and treated with 0.1 mol solution of the BTAC and CTAC surfactants, respectively. From the TG and DTA results I (see Fig. 9) it followed that the release of water and organic compounds used for the surface modification from the titania took place on heating up 560 °C.

From TG and DTA measurements of the surface modified titania xerogel samples it followed that the organic substance used for the surface modification were removed by heating up to 560°C in air. The gels annealed at temperature up to 300°C were amorphous by XRD. The diffraction peaks of anatase were observed in gels annealed at 400°C or higher temperatures. In gels annealed at 600 °C a weak peaks of rutile were found in the XRD pattern.

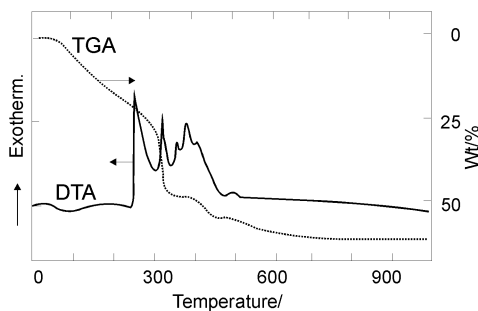
The DSA measurements of were performed for the titania gel powders calcined at 600°C (see Fig.10, a, b, c)

The increase of the radon release rate E observed on heating of the sample in the range 20-200°C (Fig. 10 a, b, c) indicated the exposure of the surface and open porosity after the release of adsorbed water. The gradual increase of E in the range 200-700 °C was ascribed to the radon diffusion along the pores of the titania xerogel.

The transport properties of the porous system towards radon (radon atoms size 0.4 nm is comparable to water molecule) were assessed after the evaluation of the DSA results by means of the mathematical model. The model curves for the radon release from the titania samples coresponding to the temperature intervals 50-400 °C and 400-950 °C are presented in Fig. 11 a, b. The relatively higher permeability was ascribed to the surface modified titania gels by means of CTAC. The break observed on the DSA curve in the range 700-750 °C with the surface modified titania gel was ascribed to the collaps of the porous system of titania due to sintering (supposedly enhanced by the crystallization of rutile). The DSA results are consistent with the surface are and pore volume of the gel samples.



a)



b)

Fig.9 TGA and DTA results of titania xerogel dried at 90°C (a) non modified by surfactants and (b) subsequently modified by CTAC surfactant

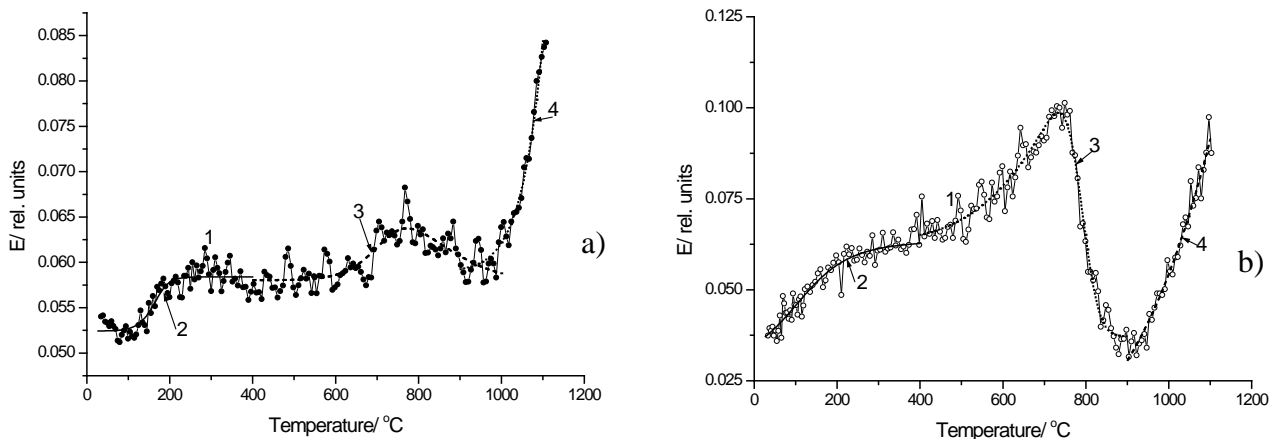


Fig.10 DSA experimental results compared with the results of mathematical modeling of titania gel powders measured on heating in argon (a) non modified by surfactants, (b) and (c) modified by treatment with the CTAC and BTAC surfactants, respectively. Curves 1 represent the experimental DSA results, curves 2-4 the model curves.

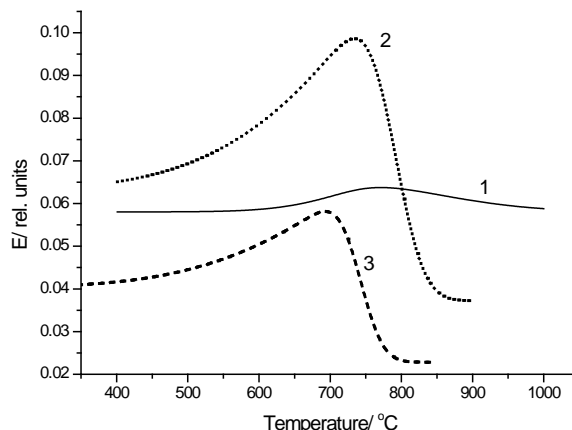
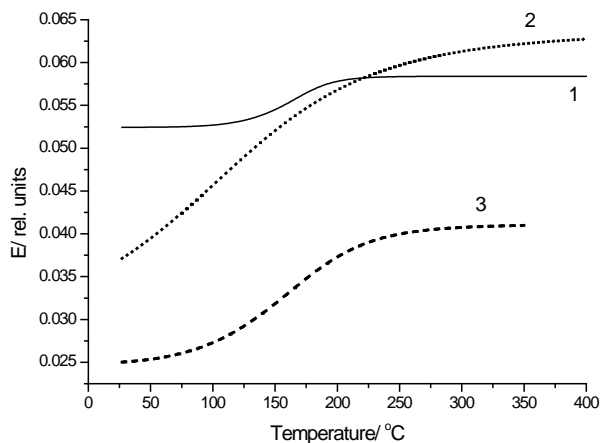
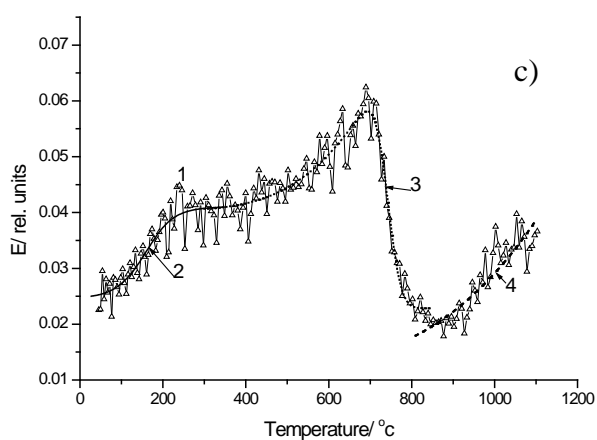


Fig.11 DSA model curves characterizing the thermal behaviour of titania gel powders (a) in the temperature ranges (a) 30-400°C and (b) 400-950 °C. Curves 1, 2, 3 correspond to the samples non treated and treated with CTAC and BTAC surfactants, respectively.

(b) Surface modified titania mesoporous films

Titania powders were prepared from the hydrolyzed alcoxide precursor and treated with 0.1mol solutions of the BTAC and CTAC surfactants, respectively. From the TG and DTA

results (see Fig.9) it followed that the release of organic compounds and water from the titania films took place on heating in air up to 560 °C.

The air dried titania films were examined by DSA under constant heating rate 6 K/min. The mass of the samples after heating decreased by 1.2-1.74 %. Figs.12.a, b, c depict the DSA experimental results (curve 1 presented as dots) as well as model curves characterizing the $\Psi(T)$ descending function (curve 2) and the model characterizing the radon diffusion by volume in sample bulk, (curve 3) observed at temperatures above 800 °C.

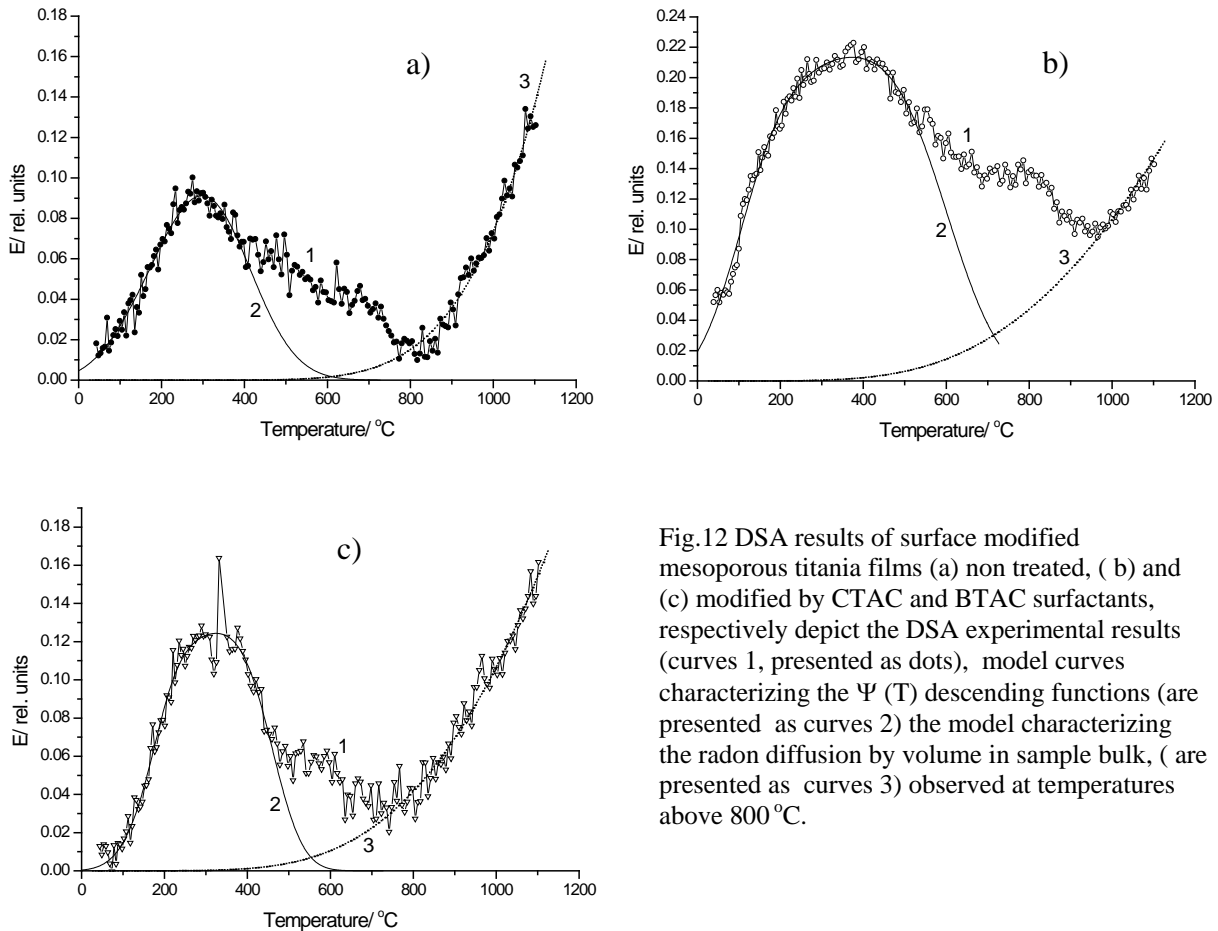


Fig.12 DSA results of surface modified mesoporous titania films (a) non treated, (b) and (c) modified by CTAC and BTAC surfactants, respectively depict the DSA experimental results (curves 1, presented as dots), model curves characterizing the $\Psi(T)$ descending functions (are presented as curves 2) the model characterizing the radon diffusion by volume in sample bulk, (are presented as curves 3) observed at temperatures above 800 °C.

It was supposed that the increase of radon release rate E in the temperature range 20-230 °C was controlled by single jump radon diffusion mechanism along the structure irregularities in the near surface layers of the titania and the annealing of the irregularities took place in the range 300-600 °C in all titania film samples. The evaluation of the annealing process by using the mathematical modeling was carried out.

The $\Psi(T)$ function, characterizing the decrease the radon diffusion channels on sample heating in air are depicted in Fig.13.

In order to compare behaviour of the titania samples in the intermediate range for every sample the model curves (denoted as curves 2 and 3 respectively) were subtracted from the DSA experimental curves (denoted as curve 1). The results of this mathematical operation are presented in Fig.14 a, b, c together with the DSA experimental results.

Obviously, by this way the microstructure changes taking place in the titania surface modified films can be better distinguished from the thermal behavior the titania gel film without surface modifications. Fig. 15 depicts the comparison of these intermediate parts of the DSA curves.

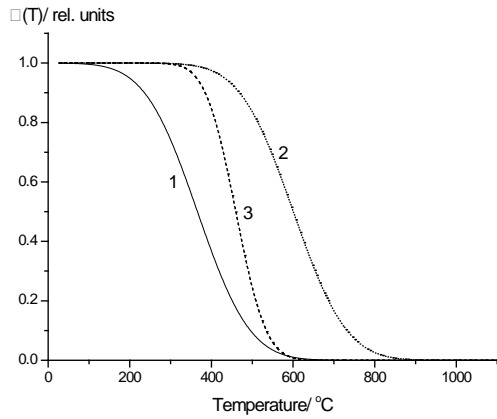


Fig.13 Temperature dependences of the $\Psi(T)$ functions, charactering the annealing of near surface irregularities serving as radon diffusion channels on air heating of the titania mesoporous samples: Curves 1- non treated, curves 2 and 3 – samples treated with CTAC and BTAC, respectively.

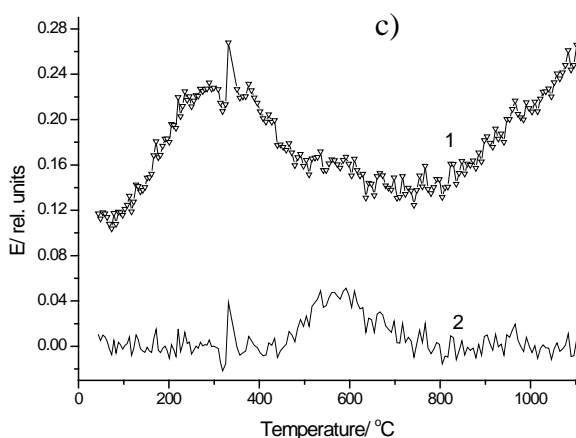
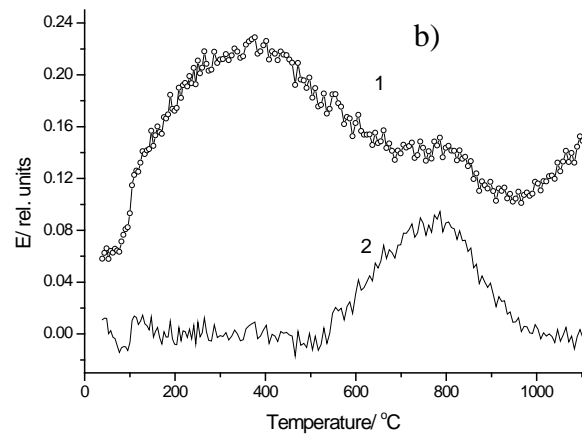
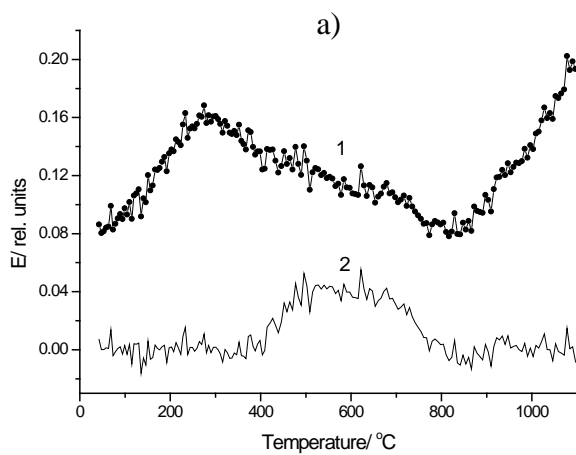


Fig.14. Comparison of the DSA experimental results (curve 1) and the remainder curves (curve 2) resulting after subtraction of the model curves, characterizing the annealing of the near surface irregularities and the bulk diffusion of radon in titania mesoporous films (a)- non treated, (b) and (c) – samples treated with CTAC and BTAC, respectively.

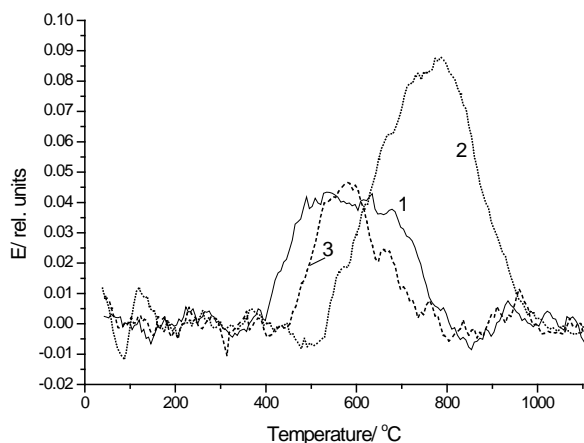


Fig. 15 depicts the comparison of the remainders obtained by mathematical treatment of the DSA curves for titania mesoporous films (a)- non treated, (b) and (c) – samples treated with CTAC and BTAC, respectively.

Characterization of the precursors for alumina based sorbents.

In cooperation with the researchers from the Institute of Inorganic Chemistry, Řež the thermal behavior of hydrargillite (aluminium hydroxide) was investigated in order to determine the temperature intervals of the formation of the intermediate product AlOOH and final Al_2O_3 , to be used as sorbent for fluor.

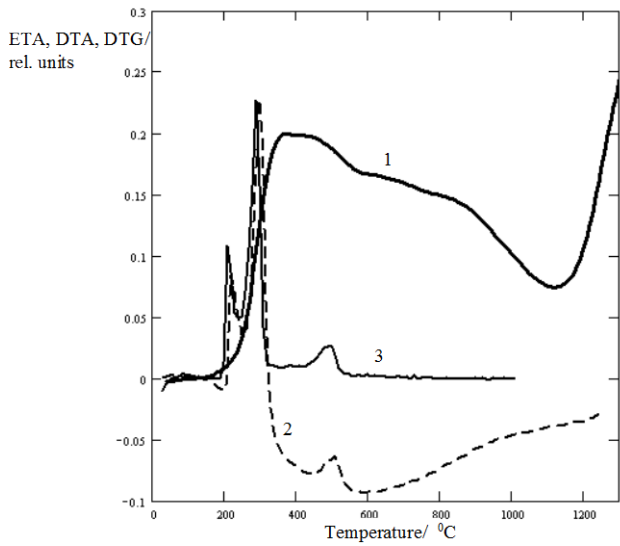
The differential thermal analysis (DTA), thermogravimetry (TG) and mass spectrometric (MS) detection of the evolved gases were used in order to elucidate the chemical processes taking place during heating of the hydrargillite.

The DSA was used in the NRI Řež with the aim to characterize the effect of the processes of thermal decomposition of $\text{Al}(\text{OH})_3$ and AlOOH on the microstructure of the intermediate products. Moreover the thermal stability of the microstructure of the resulting aluminium oxide was characterized on further heating in argon in the range up to 1100°C .

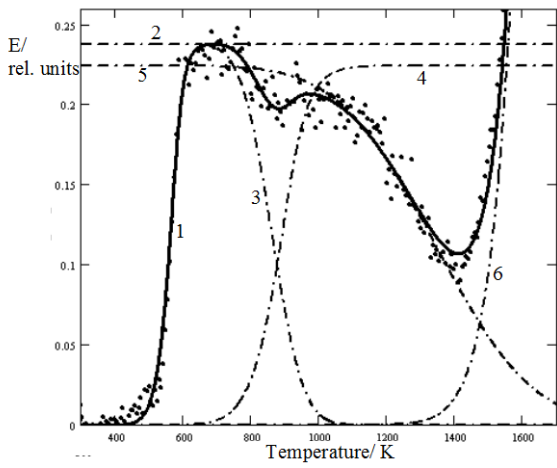
Fig. 16a presents the experimental DSA results compared with the results of DTA and DTG.

From Fig. 16 b it followed that model curves used for the evaluation of the DSA experimental results fit well with the DSA results. The model curves in Figs. 17 a, b characterize temperature dependences of the annealing of structure irregularities of hydrargillite observed by DSA in two different temperature ranges.

The DSA made it possible to characterize the increase of the surface area under *in situ* conditions of the thermal decomposition of hydrargillite mineral in the temperature range up to 320°C . On further heating above 600°C the annealing of structure irregularities in aluminium oxide was characterized by means of DSA.



a)



b)

Fig. 16 (a) Experimental results of DSA (curve 1), DTA (curve 2) and DTG (curve 3) characterizing thermal decomposition of hydrargillite. (b) Comparison of experimental DSA results with the model curves characterizing temperature dependencies of the formation and subsequent annealing of structure irregularities during heating of hydrargillite in argon.

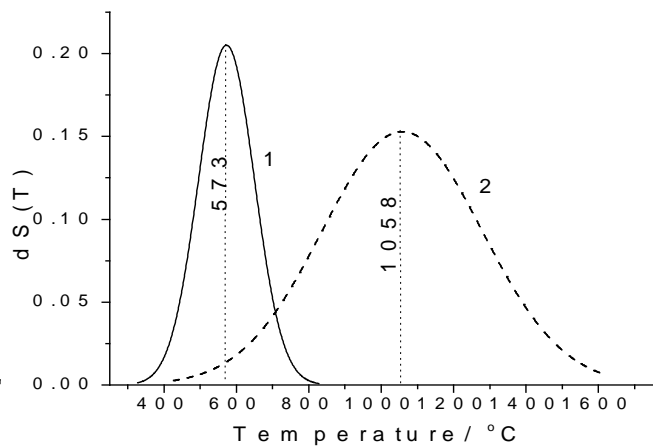
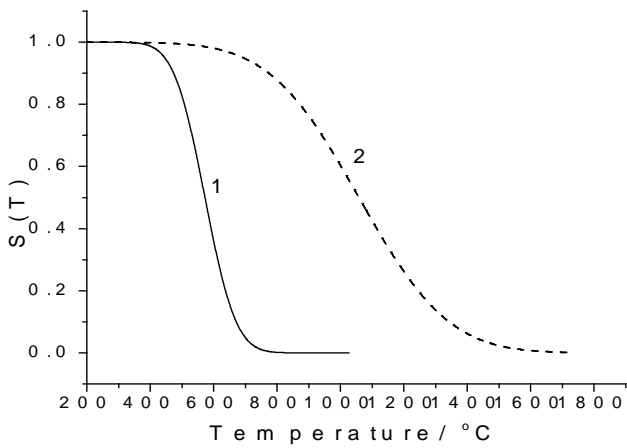


Fig. 17 Temperature dependences of the structure function $\Psi(T)$ and $d\Psi/dT$, characterizing the annealing of structure irregularities in two different temperature ranges during heating of hydrargillite.

Thermal behaviour of porous alumina gels

It was observed that the microstructure of alumina gels powders prepared by hydrolysis of alcoxides have substantial impact on their catalytic properties. Therefore, the monitoring of microstructure development on heating of the alumina gels precursors is necessary to determine optimal conditions for the preparation and subsequent treatment (e.g. drying, additional surface treatment) as well as to determine the temperature range at which the highly porous products are maintained (e.g. up to the elevated temperatures of the respective catalytic reactions).

In this study we investigated the alumina gel powders prepared by hydrolysis of alcoxides. The experimental conditions used for drying differed, in the preparation of xerogels and aerogels, respectively.

Thermal behavior of two alumina xerogel samples (without and with the additional surface treatment the CTAC surfactant, respectively) and one alumina aerogel sample were characterized by TG, DTA coupled with MS and by DSA. The results are presented in Figs 18 a,b,c.

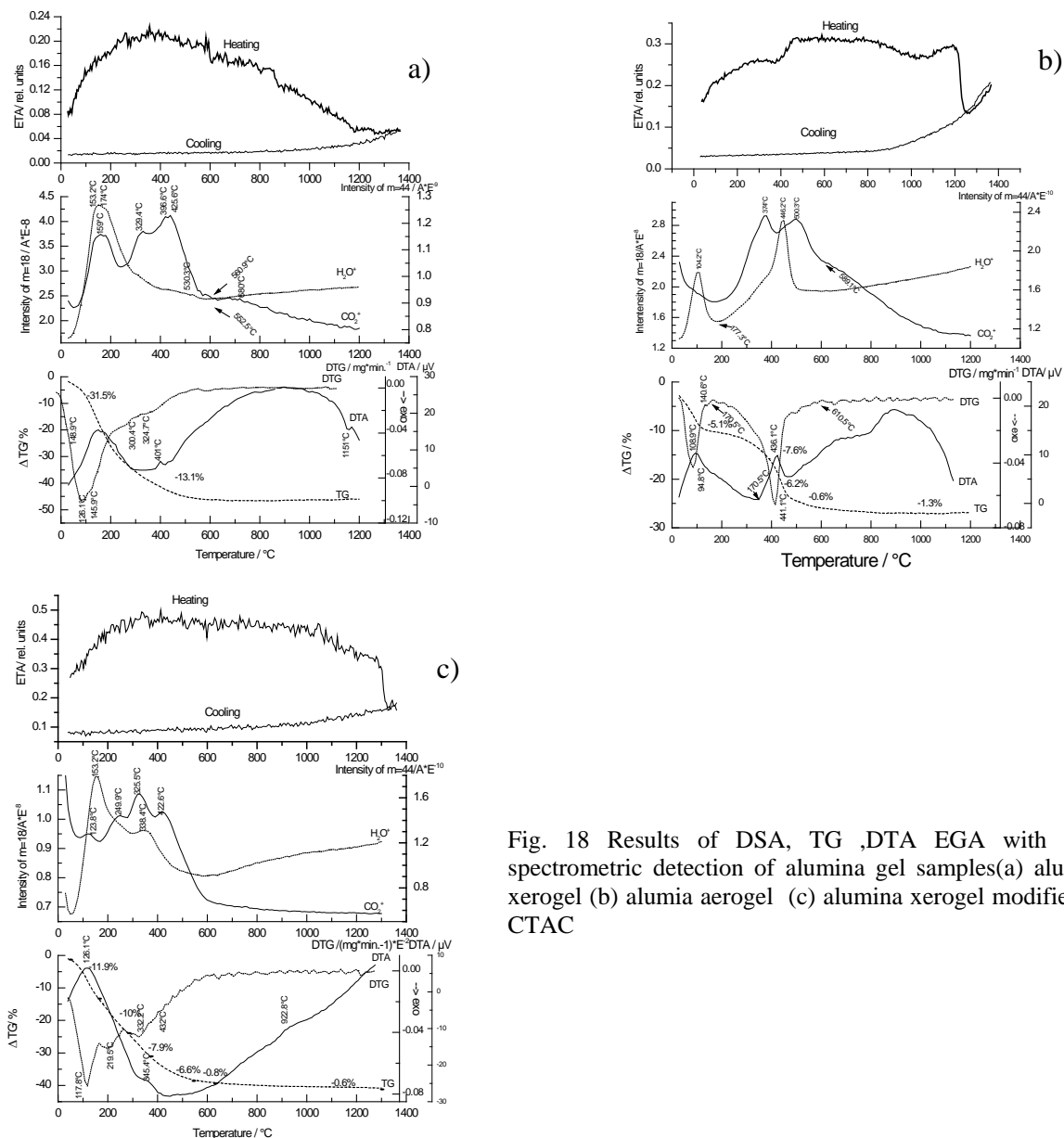


Fig. 18 Results of DSA, TG ,DTA EGA with mass spectrometric detection of alumina gel samples(a) alumina xerogel (b) alumia aerogel (c) alumina xerogel modified by CTAC

From the TG/DTA/MS results it followed that water and organic molecules were removed from the alumina gel samples after heating to 500 °C.

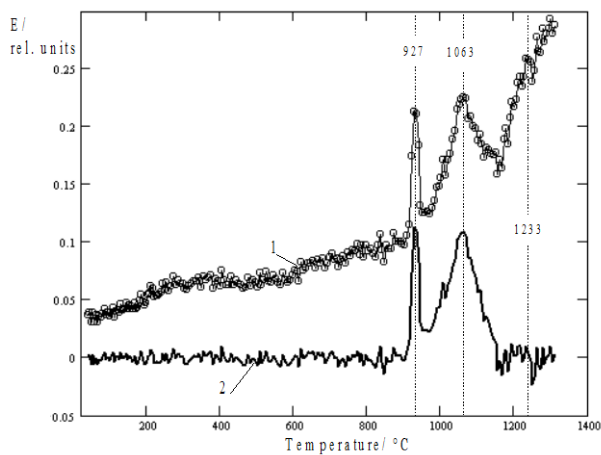
From the E values obtained by DSA at 50 °C it followed that the surface treatment of the alumina xerogel caused 2.72 fold increase of surface area as compared to the not treated alumina xerogel. The optimal temperatures for the preparation of the porous alumina gel were determined from the DSA results. The optimal temperature for the heat treatment of the aerogel precursor was recommended to be 500 °C. From the values of E_{50} and E_{500} it followed the surface area of the aerogel precursor increased 1.8 times. The temperature intervals at which the relatively highest value of E was maintained correspond to the developed porous system. The thermal stability of the respective porous system was determined from the DSA results (Figs. 18 a,b,c). From this viewpoint the lower thermal stability possess the alumina xerogel (non treated) where the E value decreased on heating above 400 °C up to 1200 °C. For surface treated alumina xerogel the stability of the porous system (characterized by larger pore radius) increased up to 1000 °C. The abrupt decrease of E above 1270 °C indicated the collapse of the porous system due to sintering. For alumina aerogel, which possessed relative stability of the porous system, the sintering was indicated at 1200°C.

Characterization of the precursors for the ruthenium oxide based catalysts.

Lanthanum-ruthenium co-precipitated hydroxide was used as precursor for ruthenium oxide based catalysts with perovskite structure. The DSA results characterizing thermal behavior of this precursor under *in situ* conditions of heating in argon were compared with the results of TG, DTA, mass spectrometric detection of the evolved gases. The results obtained during the heating of the precursor in argon are presented in Fig. 19 a, b. The XRD diffraction patterns were used in order to identify the phase compositions of the intermediate products of the thermal treatment of the precursors, such as LaRuO_3 and $\text{La}_{3.5}\text{Ru}_{4.0}\text{O}_{13}$ catalysts, which can be used in the automobile industry for the treatment of the exhaust gases in order to diminish the NO_x content.

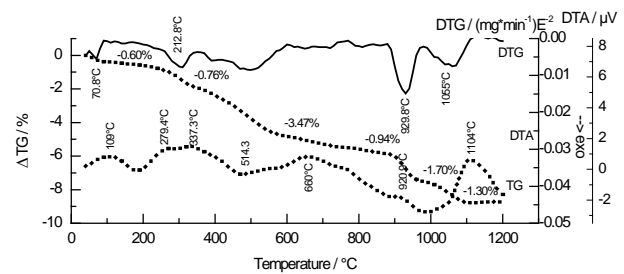
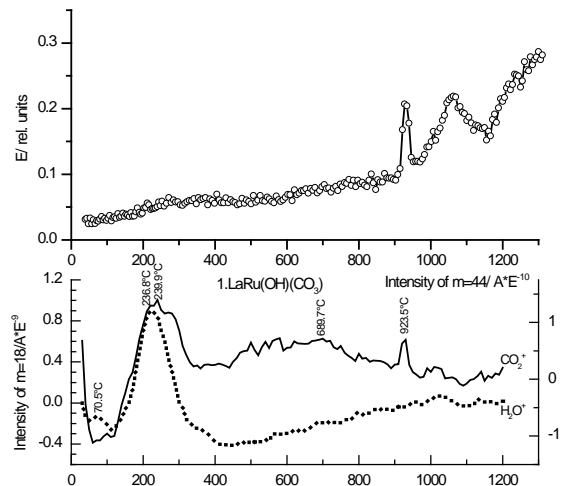
The evaluation DSA results made it possible to characterize and predict the role of the processes taking place on heating of the precursor on the development of the microstructure, which is important for the final properties of the designed catalysts.

The background equations of the mathematical model used in the mathematical evaluation of the DSA results are presented below in this report.



a)

Fig.19 Thermal behavior of La-Ru-Hydroxide during heating in argon
 (a) Experimental results of DSA (curve 1) and the DSA results obtained after mathematical treatment (curve 2) indicating the temperature intervals of the formation of perovskite phases LaRuO_3 and $\text{La}_{3.5}\text{Ru}_{4.0}\text{O}_{13}$, respectively.



b)

(b) Experimental results of DSA, TG/DTG, DTA and mass spectrometric detection of the release of H_2O , CO_2 from the samples heated in argon at the rate 6K/min

Characterization of chemical durability and thermal stability of glassy and ceramic matrices for immobilization of hazardous (radioactive) wastes

Borosilicate glasses and perovskite based ceramics prepared in different laboratories were leached at elevated temperatures in conditions recommended by IAEA with the aim to simulate the conditions of final repositories for high level radioactive waste (HLW). The leachate solutions were analysed to determine the concentrations of the leached out elements. The altered samples of glasses and ceramics were characterized by DSA on heating in argon with the aim to characterize the altered layers from the viewpoint of their permeation properties for radon atoms at elevated temperatures (radon atoms size 0.4 nm were considered comparable to the size of water molecule).

The DSA results characterizing the thermal behavior of the altered glass and ceramics samples were compared with the DSA results of the virgin samples of the respective materials (Figs. 20 a-f)

Characteristic temperatures determined by DSA, which indicated the softening of the glasses were used for the assessment of thermal stability of the glassy matrices.

In order to assess the availability of the altered glasses for the transport of species (monitored by radon migration) we calculated the differences of the integral functions limited by the DSA curves of the respective altered and pristine glass samples.

Following glass samples were characterized in the frame of this research program:

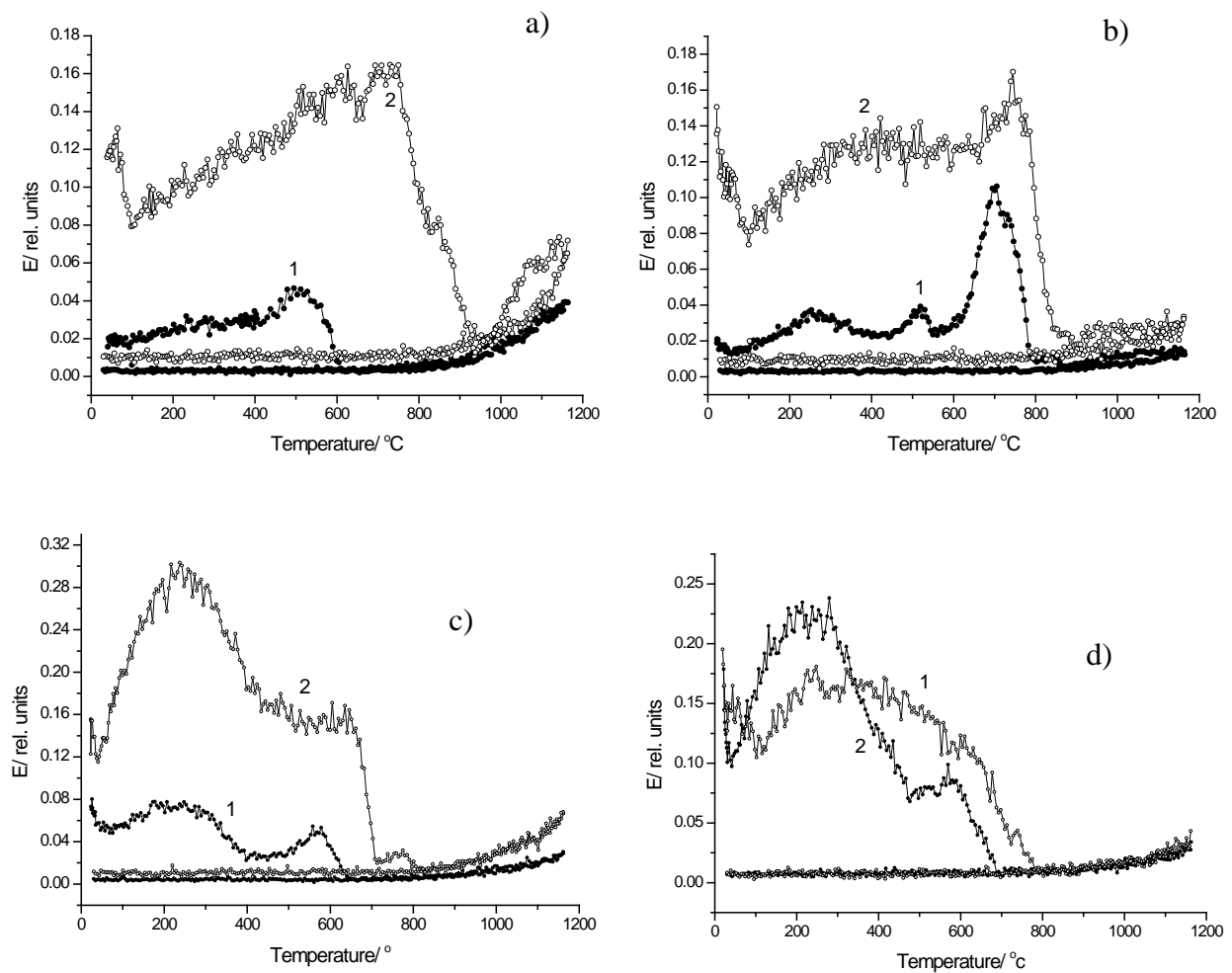
(i) Borosilicate glasses prepared at NRI Rez (Czech republic) called EXTAZA and EXPOLL designed for the immobilization of intermediate and high level radioactive waste (HLW), respectively.

(ii) Borosilicate glass for HLW prepared at HARWELL (U.K.)

(iii) Borosilicate glass of HLW designed at FZK (Germany) denoted WAK 1

(iv) Natural volcanic glass (obsidian), from the locality in New Mexico, (USA)

Fig. 20 Experimental DSA results obtained during heating and cooling of nuclear glasses and perovskite ceramics: (a). EXTAZA, (b) EXPOLL, (c) HARWELL, (d) WAK 1 (e) volcanic glass and (f) perovskite ceramics. Curves 1 – pristine forms, curves 2 – leached forms, respectively.



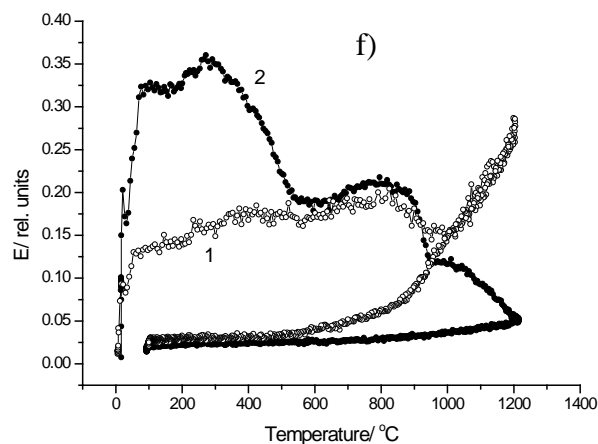
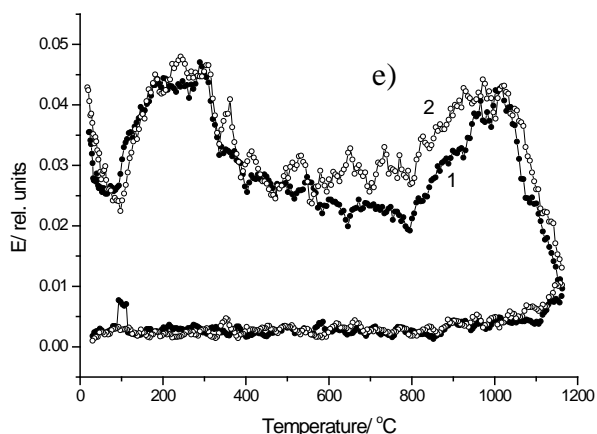


Table 1.

The characteristic parameters on the nuclear glass samples obtained by evaluation of DSA

Sample name		$T_{\text{soft}}/^{\circ}\text{C}$	$T_{\text{melt}}/^{\circ}\text{C}$	E(T) curves integral (I)	$I_{\text{Leached}}/I_{\text{pristine}}$
EXTAZA	Pristine	510	610	9.09	10.2
	Pristine	735	960	93.1	
EXPOLL	Pristine	700	750	24.9	3.7
	Leached	790	850	86.3	
HARWELL	Pristine	570	670	22.6	5.2
	Leached	650	740	118.1	
WAK-1	Pristine	580	680	68.5	1.13
	Leached	350	790	77.5	
Volcanic glass	Pristine	1000	1150	32.8	1.1
	Leached	1000	1150	36.5	

In order to assess the availability of the altered glasses for the transport of species (monitored by radon migration) we calculated the differences of the integral functions limited by the DSA curves of the respective perovskite ceramics samples denoted "as prepared" and "as leached".

Table 2

The characteristic parameters of the perovskite ceramics obtained by evaluation of DSA

Sample name		$T_{\text{onset}}/^{\circ}\text{C}$	$T_{\text{bottom}}/^{\circ}\text{C}$	E(T) curves integral (I)	$I_{\text{prepared}}/I_{\text{leached}}$
Perovskite ANSTO	as prepared	850	940	232.8	1.53
	as leached	825	990	152.2	

The perovskite ceramics was supplied by ANSTO (Australia)

Differences of the glass and ceramics samples in their thermal stability and permeability of the altered layers are obvious from Table 1.

It is interesting to point out that in the case of glassy matrices a considerably higher radon permeability can be attributed to the altered glasses. This is explained by the fact that after the leaching out metal elements and boron the alumino-silicate matrix became porous, which was reflected by the DSA as the increase of radon permeability of the altered samples.

As expected, for the obsidian (volcanic glass), which possessed very high chemical durability, no difference was observed between the DSA results of the samples before and after hydrothermal treatment

For the perovskite ceramics, in contrary the “as sintered” ceramic sample was characterized by higher porosity and permeability for radon that the sample submitted to hydrothermal treatment.

Conclusions.

The research work carried out in the frame of my study stay was fulfilled.

The comparison of the results of different methods gave us the information important for the assessment and prediction of the behavior of the intermediate products of the new ecological materials. These results will be used for the optimization of technological conditions for preparation of new ecological materials.

Several publications, based on the research obtained under my participation, will be published.

A copy of one paper to be published in Journal of thermal analysis and calorimetry is attached to this report.

Acknowledgment

I wish to express thanks to the NATO Science fellowship program for the financial support of my stay at the NRI Rez and to the host institute for the good working conditions for my research work.

I.M. Bountseva